Molecular Neurobiology (2019) 56:8237–8254
https://doi.org/10.1007/s12035-019-01657-y

Megalencephalic Leukoencephalopathy with Subcortical Cysts Protein-1 (MLC1) Counteracts Astrocyte Activation in Response to Inflammatory Signals

Maria Stefania Brignone[1] · Angela Lanciotti[1] · Barbara Serafini[1] · Cinzia Mallozzi[1] · Marco Sbriccoli[1] · Caterina Veroni[1] · Paola Molinari[2] · Xabier Elorza-Vidal[3] · Tamara Corinna Petrucci[1] · Raul Estévez[3,4] · Elena Ambrosini[1]

Received: 15 February 2019 / Accepted: 20 May 2019 / Published online: 17 June 2019

Abstract

Megalencephalic leukoencephalopathy with subcortical cysts protein-1 (MLC1) is a membrane protein expressed by perivascular astrocytes. MLC1 mutations cause MLC, an incurable leukodystrophy characterized by macrocephaly, brain edema, cysts, myelin vacuolation, and astrocytosis, leading to cognitive/motor impairment and epilepsy. Although its function is unknown, MLC1 favors regulatory volume decrease after astrocyte osmotic swelling and down-regulates intracellular signaling pathways controlling astrocyte activation and proliferation. By combining analysis of human brain tissues with in vitro experiments, here we investigated MLC1 role in astrocyte activation during neuroinflammation, a pathological condition exacerbating patient symptoms. MLC1 upregulation was observed in brain tissues from multiple sclerosis, Alzheimer's, and Creutzfeld-Jacob disease, all pathologies characterized by strong astrocytosis and release of inflammatory cytokines, particularly IL-1β. Using astrocytoma lines overexpressing wild-type (WT) or mutated MLC1 and astrocytes from control and *Mlc1* knock-out (KO) mice, we found that IL-1β stimulated WT-MLC1 plasma membrane expression in astrocytoma cells and control primary astrocytes. In astrocytoma, WT-MLC1 inhibited the activation of IL-1β–induced inflammatory signals (pERK, pNF-kB) that, conversely, were constitutively activated in mutant expressing cells or abnormally upregulated in KO astrocytes. WT-MLC1^{+} cells also expressed reduced levels of the astrogliosis marker pSTAT3. We then monitored MLC1 expression timing in a demyelinating/remyelinating murine cerebellar organotypic culture model where, after the demyelination and release of inflammatory cytokines, recovery processes occur, revealing MLC1 upregulation in these latter phases. Altogether, these findings suggest that by modulating specific pathways, MLC1 contributes to restore astrocyte homeostasis after inflammation, providing the opportunity to identify drug target molecules to slow down disease progression.

Keywords Leukodystrophy · Neuroinflammation · Neurodegeneration · IL-1β · pERK · Astrocytosis

Brignone Maria Stefania and Lanciotti Angela contributed equally to this work.

Electronic supplementary material The online version of this article (https://doi.org/10.1007/s12035-019-01657-y) contains supplementary material, which is available to authorized users.

✉ Elena Ambrosini
elena.ambrosini@iss.it

[1] Department of Neuroscience, Istituto Superiore di Sanità, Viale Regina Elena 299, 00161 Rome, Italy

[2] Department of FARVA, Istituto Superiore di Sanità, Viale Regina Elena 299, 00161 Rome, Italy

[3] Unitat de Fisiologia, Departamento de Ciències Fisiològiques, IDIBELL-Institute of Neurosciences, Universitat de Barcelona, L'Hospitalet de Llobregat, Spain

[4] Centro de Investigación en Red de Enfermedades Raras (CIBERER), ISCIII, Valenciana, Spain

Introduction

In the central nervous system (CNS) astrocytes exert several important functions for the maintenance of brain homeostasis, including metabolic support for neurons, spatial buffering of extracellular K^{+} ions, neurotransmitter uptake, formation and maintenance of the blood-brain barrier (BBB), and regulation of the brain immune response [1]. Alterations of brain homeostatic conditions lead to astrocyte "activation," a multi-staged, finely regulated pathophysiological process characterized by typical morphological and functional hallmarks [2–4]. Astrocyte activation is mainly needed to protect the CNS from insults, but can be detrimental if not controlled. Reactive

astrocytes have been observed in almost all brain pathologies (i.e., stroke, trauma, epilepsy), including inflammatory and neurodegenerative diseases, where, even though not primarily culprits, astrocytes play an important role in disease initiation, progression, and resolution [2, 5–8]. Recently, mutations in astrocytic specific proteins proved to be the primary cause of the myelin defects and neurodegeneration observed in some genetic leukodystrophies (reviewed in [9]), among which the megalencephalic leukoencephalopathy with subcortical cysts disease (MLC). This rare disease is clinically characterized by macrocephaly, ataxia, spasticity, motor and cognitive decline, and seizures [10–12]. Brain edema, subcortical cysts, myelin vacuolation, and reactive astrocytosis have been observed in the brain of MLC patients by MRI and histological analysis of tissue biopsies [13–15].

Although the precise function of MLC1 protein is still elusive, both MLC neuropathological features (white matter edema and fluid cysts) and experimental evidences from pathological models [defects of swelling-induced chloride current and regulatory volume decrease (RVD)] suggest that MLC1 mutations alter the capacity of astrocytes to control ion and fluid exchanges and cell volume variations [16, 17].

In the CNS, temporary astrocyte swelling occurs physiologically in response to neuronal activity and extracellular K^+ release, but it is also a consequence of astrocyte activation following brain damage and inflammation [18–20]. Altogether, these observations lead to hypothesize that MLC1, by favoring the RVD needed to rescue normal cell volume, is involved in the control/inhibition of astrocyte activation in different pathological conditions. Consequently, MLC1 functional defects could lead to abnormal astrocyte reaction in response to insults and/or changes of brain homeostatic conditions.

Reactive astrocytes observed in brain biopsies [13–15] and aggravation of clinical symptoms occurring in patients after fever or mild trauma [14, 21, 22] are consistent with this latter hypothesis. Accordingly, we previously demonstrated that in human U251 astrocytoma cells, MLC1 expression inhibited the activation of epidermal growth factor receptor (EGFR), extracellular signal-regulated kinase (ERK) 1/2 and phospholipase C gamma (PLC-γ) [23], all components of an intracellular signaling cascade involved in the proliferation and activation of astrocytes in response to brain damage [2, 24, 25]. In the same cells, WT MLC1 also inhibited the functionality of KCa3.1 [23], the calcium-activated potassium channel selectively expressed by astrocytes at the BBB and involved in astrogliosis and neuroinflammation [26, 27]. Noteworthy, increased ERK phosphorylation was observed in cultured astrocytes obtained from *Mlc1* KO mice, when compared to astrocytes derived from wild-type animals [28]. Additionally, studies performed using in vitro differentiated macrophages derived from peripheral blood monocytes, a cellular type expressing MLC1 protein outside the brain, indicated that MLC1 pathological mutations strongly impair cell response to inflammatory stimuli [29].

Based on these findings, by combining the analysis of human brain tissues with in vitro experiments, here we explored the possibility that MLC1 has a role in the processes regulating astrocyte activation in neuroinflammatory conditions and that alterations of this function may contribute to the pathogenic mechanisms of MLC disease.

Materials and Methods

Immunohistochemistry of Human Brain Tissues

Multiple Sclerosis Patients and Tissues

Double indirect immunofluorescence stainings for major histocompatibility complex (MHC) class II molecules and MLC1 were performed on ten-micrometer-thick sections cut from snap frozen brain tissues from four cases with secondary progressive multiple sclerosis (MS) and two cases deceased for non-neurological pathologies. Tissues were obtained by the UK Multiple Sclerosis Tissue Bank at the Imperial College of London after collection via a prospective donor program with fully informed consent. The use of post-mortem human brain material was approved by the Ethics Committee of Istituto Superiore di Sanità (ISS). Demographic and clinical characteristics of the cases analyzed are provided in Table 1. The MS tissue blocks used for this study contained subcortical white matter (WM) with lesions characterized by normal or rarefied myelin and diffuse microglial activation in the absence of prominent perivascular leukocyte infiltration, and areas of normal appearing white matter (NAWM).

Immunofluorescence Stainings on MS and Control Brain

Double immunofluorescence (IF) stainings of 10-μm thick brain sections were carried out as follows: after drying for 2 hours (h) under chemical hood, sections were fixed in cold acetone for 10 minutes (min) and then dried for 10 min at room temperature (RT). After rehydration in PBS, sections were incubated with 10% normal goat serum (NGS) (Sigma-Aldrich, St Louis, MO) in PBS 1 h at RT and then overnight (ON) at 4 °C with a mixture of rabbit anti-MLC1 polyclonal antibody (pAb, 1:200; Atlas AB, AlbaNova University Center, Stockholm, Sweden) and mouse anti-human HLA-DP, DQ, DR antigen monoclonal antibody (mAb, 1:50; clone CR3/43, DakoCytomation, Denmark) in PBS containing 1% of Bovine Serum Albumin. A mixture of Alexa fluor-488 conjugated goat anti-mouse IgG and tetramethylrhodamine (TRITC)-conjugated goat anti-rabbit IgG secondary Abs (all from Jackson ImmunoResearch) diluted in PBS + 3% NGS was subsequently applied for 1 h at RT. After further washings, sections were mounted with anti-fade mounting medium with DAPI (Invitrogen). Negative control stainings were

Table 1 Demographic, clinical, autopsy, and neuropathological details of the MS and control cases analyzed

Case	Sex/age at death (years)	Age at onset (years)	Disease duration (years)	Cause of death[b]	Post-mortem delay (hours)
MS180	F/44	26	18	MS	9
MS79	F/49	25	24	MS	7
MS342	F/35	30	5	MS	9
MS160	F/44	29	15	MS	18
C25	M/35			Carcinoma of the tongue	22
C45	M/77			Myocardial degeneration/-bronchopneumonia	22

[a] All MS cases analyzed were in the secondary progressive phase of the disease

[b] MS is stated as a cause of death where death occurred as a direct result of MS or any related disability

performed using Ig isotype control (mouse IgG1k) and rabbit pre-immune serum. Sections were finally analyzed and images acquired with a digital epifluorescence microscope (Leica Microsystem, Wetzlar, Germany).

Creutzfeldt-Jakob and Alzheimer's Disease Patients and Tissues

Paraffin blocks of brain samples from sporadic Creutzfeldt-Jakob and Alzheimer's disease patients and control subjects present in the tissue archive of the Department of Neuroscience of the ISS were used for this study. Their diagnoses were established by clinical data, histological examination, immunohistochemical stainings, and biochemical analyses. The use of post-mortem human brain material was approved by the ISS Ethics Committee.

Immunohistochemistry and Double Immunofluorescence Stainings on Creutzfeldt-Jakob and Alzheimer's Disease Brain Samples

Five-micrometer-thick sections of frontal cortex were cut on microtome and collected onto glass slides for immunohistochemical analysis. For bright field immunohistochemistry, paraffin-embedded sections were deparaffinized, rehydrated in descending graded alcohols, incubated for 10 min in methanol containing 3% hydrogen peroxide to block endogenous peroxidase activity, and then subjected to heat-induced antigen retrieval by microwaving in 10 mM sodium citrate buffer (pH = 6). After pre-incubation in diluted NGS for 1 h, sections were incubated ON with rabbit anti-MLC1 pAb (1:250; Atlas AB) at 4 °C in humid chambers. Slides were then washed with PBS, incubated with biotinylated anti-rabbit secondary Ab (1:200; Vector Laboratories) in PBS for 1 h at RT, and then with the avidin–biotin-peroxidase complex (Vectastain ABC-Elite kit, Vector Laboratories), according to the manufacturer's instructions. Sections were then stained with 3′-3′-diaminobenzidine (DAB, Sigma) substrate chromogen to visualize the reaction products and finally counterstained with hematoxylin (Bio-Optica, Italy). A Leica DM2100 microscope was used for slide examination and image acquisition. For double IF stainings paraffin-embedded sections, treated as previously described, were incubated ON at 4 °C in humid chamber with a mixture of rabbit anti-MLC1 pAb (1:250, Atlas AB) and mouse anti-GFAP mAb (1:100, Dako, Denmark) as primary Abs. Slides were subsequently washed with PBS and incubated for 1 h with a mixture of Alexa fluor-488 conjugated goat anti-mouse IgG (1:200, Jackson ImmunoResearch) and TRITC-conjugated goat anti-rabbit IgG (1:150) secondary Abs diluted in PBS + 3% NGS. Sections were then washed, mounted with anti-fade Vectashield mounting medium (Vector Laboratories, Inc., Burlingame, CA) and analyzed with a laser scanning confocal microscope (LSM 5 Pascal, Carl Zeiss, Jena, Germany).

Cell Cultures and Treatments

Astrocyte-enriched cultures (about 95% of purity) were obtained from 1- or 2-day-old newborn rats and maintained in culture as previously described [30]. Astrocytes derived from wild-type (wt) and *Mlc1* knock-out (KO) mice were generated and cultured as previously indicated in Duarri et al. 2011; [15]. U251 astrocytoma cell lines infected with an empty retroviral vector (mock-infected U251 cells, Ø) or with a vector stably expressing recombinant MLC1 WT or carrying the S280L pathological mutation were obtained and grown as previously described [31]. When indicated, astrocytoma cells and primary rat/mouse astrocytes were stimulated ON with 1, 10, and 50 ng/ml of interleukin-1 beta (IL-1β, Labome) and used for immunofluorescence stainings, Western blot (WB) analysis, and real-time PCR, as described below.

Protein Extract Preparation and Western Blotting

Protein fractions from human astrocytoma and rat and mouse astrocytes were obtained as previously described [31, 32]. Equal amounts of proteins (30 μg) were resolved on SDS–PAGE using gradient (4–12%) pre-casted gels (Invitrogen), and transferred onto a nitrocellulose membrane. Membranes were blotted ON at 4 °C using the following primary Abs: anti-MLC1 pAb (1:1500; in-house generated; [33]), anti-β-actin mAb (1:2000; Santa Cruz Biotecnology), anti-phospho-EGFR mAb (1:1000; Abcam), anti-phospho-Akt (Ser473) pAb (1:1000; Cell Signaling Technology), anti-phospho-ERK1/2 (Thr202/Tyr204) mAb (1:1000; Cell Signaling Technology), anti-ERK1/2 pAb (1:1000; Cell Signaling Technology), and anti-phospho-NF-kB p65 (Ser536) mAb (1:1000; Cell Signaling Technology) in PBS+3% BSA. Anti-phospho-STAT3Tyr705 (Y705) pAb (1:1500; Cell Signaling Technology) was incubated in PBS+5% BSA and 0.1% Tween-20. Following extensive washings, membranes were incubated for 1 h at RT with secondary Abs: horseradish peroxidase-conjugated anti-mouse or anti-rabbit (1:5000; Bio-Rad). Immunoreactive bands were visualized using an enhanced chemiluminescence reagent (Thermo Scientific), according to the manufacturer's instructions, and exposed on X-ray films. Densitometric analysis of WB bands was performed using ImageJ software.

Immunofluorescence Stainings of Cultured Astrocytes

Astrocytoma cells grown on polylysine-coated coverslips were treated ON with 10 ng/ml of IL-1β, fixed for 10 min with 4% paraformaldehyde (PFA), and washed with PBS. After 1 h of incubation with blocking solution (5% BSA in PBS), cells were incubated 1 h at RT with the anti-MLC1 pAb (1:50; Atlas AB) diluted in PBS+0.025% Triton X-100. As secondary Ab, TRITC-conjugated goat anti-rabbit IgG (1:150, Jackson ImmunoResearch) was used. Coverslips were mounted with anti-fade mounting medium with DAPI (Invitrogen) and analyzed with a laser scanning confocal microscope (LSM 5 Pascal, Carl Zeiss, Jena, Germany). NIH ImageJ software (http://rsb.info.nih.gov/ij/) was used for IF quantification by means of threshold fluorescence intensity analysis within a region of interest corresponding to a single-cell profile. To confirm MLC1 protein translocation at astrocyte plasma membrane in response to IL-1β treatment, the distribution of immunofluorescence pixel intensity along a freely defined line spanning the whole cell (plasma membrane-cytoplasm-plasma membrane) was also evaluated using the profile analysis tool of the LSM 5 PASCAL.

Biotinylation Assay for the Affinity Purification of Plasma Membrane Proteins

Four 75-cm^2 flasks of 90–95% confluent astrocytoma cell lines overexpressing WT or S280L MLC1, untreated or treated ON with 10 ng/ml of IL-1β, were used for the biotinylation assay as previously described [33]. Briefly, cells were incubated with Sulf-NHS-SS-Biotin (0.25 mg/ml, Thermo Scientific, Rockford, IL) 30 min at 4 °C. The biotinylation reaction was terminated by the addition of 500 μl of Quenching solution (Thermo Scientific) per flask. Cells were then washed in PBS, harvested, and solubilized in lysis buffer (Thermo Scientific). Cells were further disrupted by brief sonication and centrifuged 2 min at 10,000 ×*g*. Solubilized biotinylated membrane proteins were incubated for 1 h at RT with NeutrAvidin® Agarose (Thermo Scientific) in column, as indicated by the manufacturer. The NeutrAvidin® Agarose bound biotinylated proteins were eluted from the column with 450 μl SDS-PAGE Sample Buffer (62.5 mM Tris-HCl, pH 6.8, 1% SDS, 10% glycerol, 50 mM DTT). Eluted protein fractions were analyzed by WB as described above. The lack of the cytoplasmic MLC1 component (36 kDa MW protein, [34]) among the eluted membrane proteins represents the negative control confirming the efficiency of the purification procedure.

Total RNA Extraction and Real-Time RT-PCR

Primary rat astrocytes Total RNA derived from primary astrocytes with or without IL-1β treatment (1, 10, and 50 ng/ml) was purified using SV Total RNA Isolation System (Promega, Madison, WI, USA). To carry out the reverse transcriptase (RT) reaction, AMV Reverse Transcriptase (Promega) was used employing oligo (dT)15 primers, according to the manufacturer's instructions. cDNA was than analyzed in triplicate by real-time PCR, using the ABI PRISM 7500 Real Time PCR, Taqman Gene Expression Master Mix and Taqman gene expression assays for both rat MLC1 [assay ID:Rn01407615_m1] and rat Actin-beta [assay ID: Rn00667869_m1] (all purchased from Life Technologies). The relative amount of MLC1 transcript was calculated normalizing to the internal control β-actin using the $2^{-\Delta Ct}$ formula.

Organotypic cerebellar slice cultures Three hundred and fifty-micrometer-thick cerebellar slices were prepared from the cerebellum of P10 CD1 Swiss mice, using previously described methods [35]. Slices were cultured for 7 days replacing fresh medium after the first day and every 2–3 days and then treated or not with lysolecithin (0.5 mg/ml; Sigma-Aldrich) for 16 h; then, the toxin was removed and fresh medium was added. Both treated and untreated slices were collected at the indicate time-points (0 h, 2 days, and 4 days after toxin removal) for gene expression analysis. Total RNA was extracted using

RNeasy Mini kit (QIAGEN, Valencia, CA), reverse transcribed using High Capacity Reverse Transcription kit (Life Technologies, Grand Island, NY) and then analyzed in triplicate by real-time PCR, using the ABI PRISM 7500 Real Time PCR, Gene Expression Master Mix and Taqman gene expression assays (all from Life Technologies). The amount of MLC1 (MLC1 specific assay code: Mm00453827_m1) transcript was calculated normalizing to the internal control GAPDH (GAPDH For: ACC CAC CCC AGC AAG GA; GAPDH Rev: GAA ATT GTG AGG GAG ATG CTC AGT; GAPDH Probe: VIC-AAG AGA GGC CCT ATC C-MGB). For each experimental point, two cerebellar slices were used in three independent experiments.

Statistical Analysis

All the statistical analyses were performed using GraphPad prism software. Results are expressed as mean values ± standard error of the mean (SEM). Data were first subjected to normality test (D'Agostino and Pearson Omnibus Normality test); when data followed a normal distribution, a Student *t* test was applied; otherwise, non-parametric tests, such as Wilcoxon test or Kruskal-Wallis test, were used. The test used is indicated in the corresponding legend of each figure.

Results

MLC1 Is Upregulated In Vivo in Neurodegenerative Diseases Characterized by Astrocyte Activation and Neuroinflammation

We and others previously reported that the expression of MLC1 protein in astrocyte endfeet surrounding blood vessels was increased in active demyelinating white matter (WM) lesions present in the autoptic brain tissue of patients affected by multiple sclerosis (MS) [36, 37] and Supplementary Material Fig. 1], the most common inflammatory demyelinating disease of the CNS characterized by variable degrees of inflammation, strong gliosis, neurodegeneration, and edema [36]. MLC1 upregulation in MS active lesions, where reactive astrocytes, foamy macrophages, and perivascular T lymphocyte infiltrates are present [37], suggests that this protein might be involved in the response of astrocytes to inflammatory signals released by immune cells. Here, we further investigated MLC1 expression in neuroinflammatory conditions, in response to signals released by intraparenchymal cells [20], before immune cell infiltration. These studies may shed light on new MLC1 functional properties and on MLC pathological mechanisms.

To this aim, MLC1 expression was analyzed by immunofluorescence in snap frozen brain sections from two patients deceased for non-neurological diseases and three MS patients containing: (i) WM areas characterized by almost intact myelin, absence of a prominent leukocyte infiltration, and strong, diffuse activation of the resident microglial cells, evaluated by MHC class II molecule expression, and (ii) normal appearing white matter (NAWM), where MHC class II expression on microglia and perivascular macrophages was very low or absent.

Double immunofluorescence stainings of control sections using MHC class II and MLC1 Abs showed an almost total absence of MHC II immunoreactivity throughout the WM and confirmed the expression of MLC1 around some large intraparenchymal blood vessels, as previously reported [34, 38], (Fig. 1a, b). When compared to control samples, all the MS tissue blocks analyzed showed an increased immunoreactivity for MLC1 (Fig. 1c–f) that was particularly evident in the WM areas characterized by a marked and diffuse expression of MHC class II on microglial cells and some perivascular macrophages. In these areas, MLC1 staining markedly increased in astrocytes contacting blood vessels and in several parenchymal cells morphologically identifiable as reactive astrocytes (Fig. 1c–f). Noteworthy, only in WM areas enriched in activated microglia, MLC1 expression was detectable around numerous small-caliber vessels throughout the lesions (Fig. 1d, e, arrows). Tight contacts between MHC class II-positive microglial cells and MLC1 expressing astrocytes were frequently observed (Fig. 1g, arrows).

We then investigated MLC1 expression in other neurodegenerative diseases characterized by a significant glial cell activation and neuroinflammation, without primary leukocyte involvement: Alzheimer's disease (AD) and Creutzfeld-Jacob disease (CJD), [39–42]. To this aim, immunostainings for MLC1 were performed on paraffin sections containing two different brain areas from a control subject (Fig. 2a, b) and from donors affected by AD (Fig. 2c, d) or CJD (Fig. 2e, f). When compared to control tissues, where MLC1 was barely detectable in the subpial region (Fig. 2a, b), we observed a strong increase of perivascular MLC1 expression around large- and small-caliber blood vessels in both AD and CJD tissue samples (Fig. 2c–f, arrows). Double immunofluorescence stainings for MLC1 and glial fibrillary astrocyte protein (GFAP) in control (Fig. 3a–c) and pathological tissues from AD (Fig. 3d–f) and CJD (Fig. 3g–i) confirmed MLC1 expression in astrocytes contacting some large blood vessels in control samples (Fig. 3a–c, arrow) and showed a significant increase of MLC1 immunoreactivity in GFAP positive astrocytes surrounding large- and small-caliber vessels (Fig. 3d–i, arrows and arrowheads, respectively) in both AD and CJD brain sections. Particularly, in CJD tissues hypertrophic $MLC1^{+}/GFAP^{+}$ cells, identifiable as reactive astrocytes, contacting small-caliber vessels were frequently detected (inset in Fig. 3i). When AD tissue samples were co-immunostained with anti-MLC1 Ab and the Ab recognizing the amyloid βA4 protein, the main component of AD plaques,

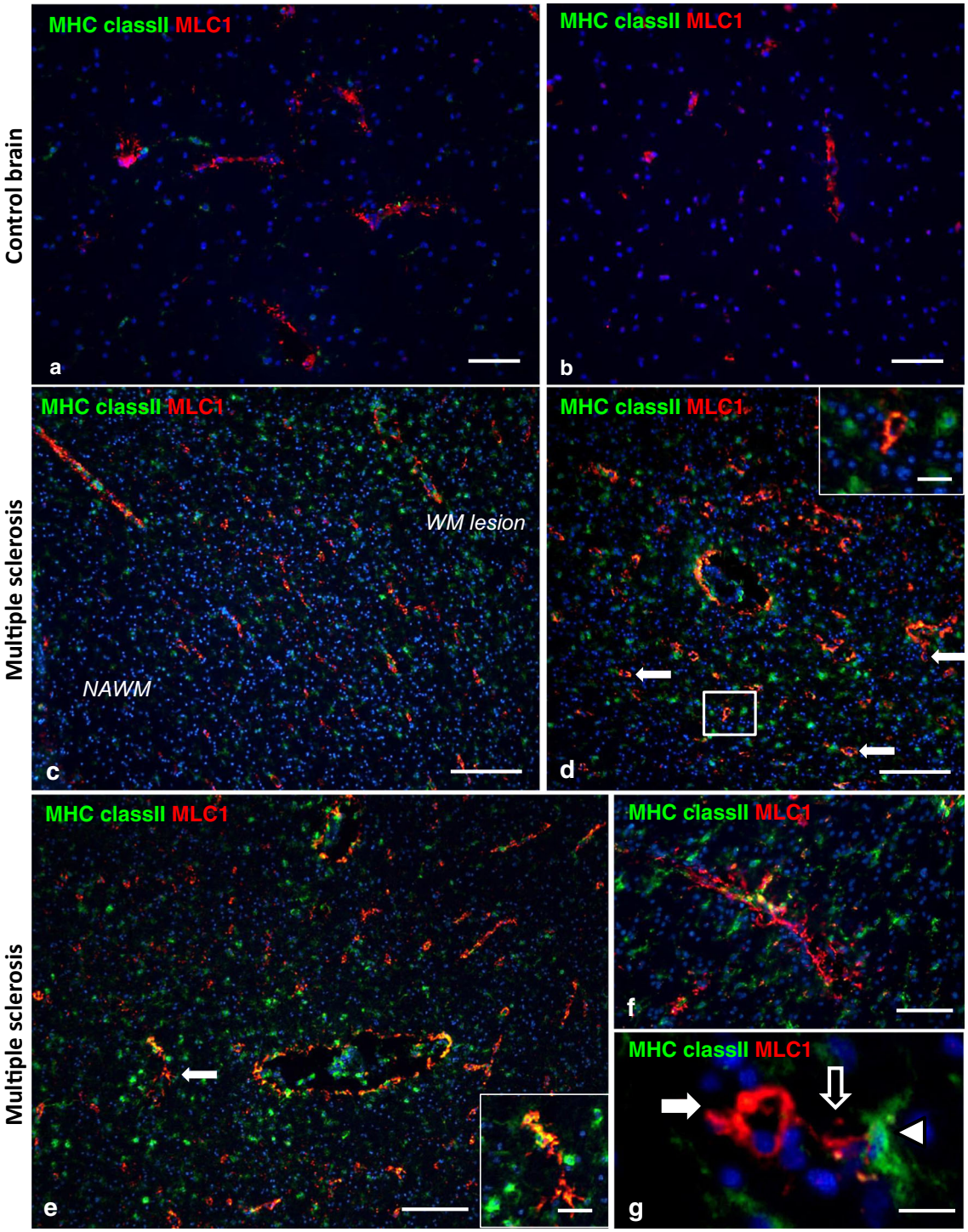

Fig. 1 MLC1 immunoreactivity in subcortical normal white matter (WM) and in WM lesions of multiple sclerosis brains. Double immunofluorescence stainings for MHC class II (green) and MLC1 (red). **a**, **b** In two control brains, MLC1 immunoreactivity is present at some blood vessels in subcortical WM, in absence of detectable MHC class II expression. **c**–**g** Three subcortical WM lesions characterized by marked and diffuse MHC class II immunoreactivity, without a prominent leucocyte infiltration and demyelination, from two MS cases (MS 180 and MS 160 cases) are shown. Compared to the adjacent normal appearing white matter (NAWM; MS180 case) increase MLC1 immunoreactivity is observed around blood vessels and in some reactive astrocytes in WM lesion, where MHC class II-expressing microglial cells and perivascular macrophages have been detected (**c**). Panels **d**–**g** show two lesions in MS 160 case: arrows in **d** point to numerous small-caliber vessels expressing MLC1 throughout the lesion, one of which (boxed area) is shown at high power magnification in the inset; inset in **e** shows at high magnification a reactive astrocyte expressing MLC1 (arrow). Panel **f** shows MLC1-positive perivascular astrocyte end-feet surrounded by activated MHC class II-positive microglia. In panel **g**, an astrocyte expressing MLC1 (empty arrow) and contacting a 15-μm diameter brain vessel (arrow) is also in tight contact with a MHC class II^+ microglial cell (arrowhead). Bars: 100 μm in **c**–**e**; 50 μm in **a**, **b**, and **f**; 20 μm in the insets in **d** and **e**; 10 μm in **g**

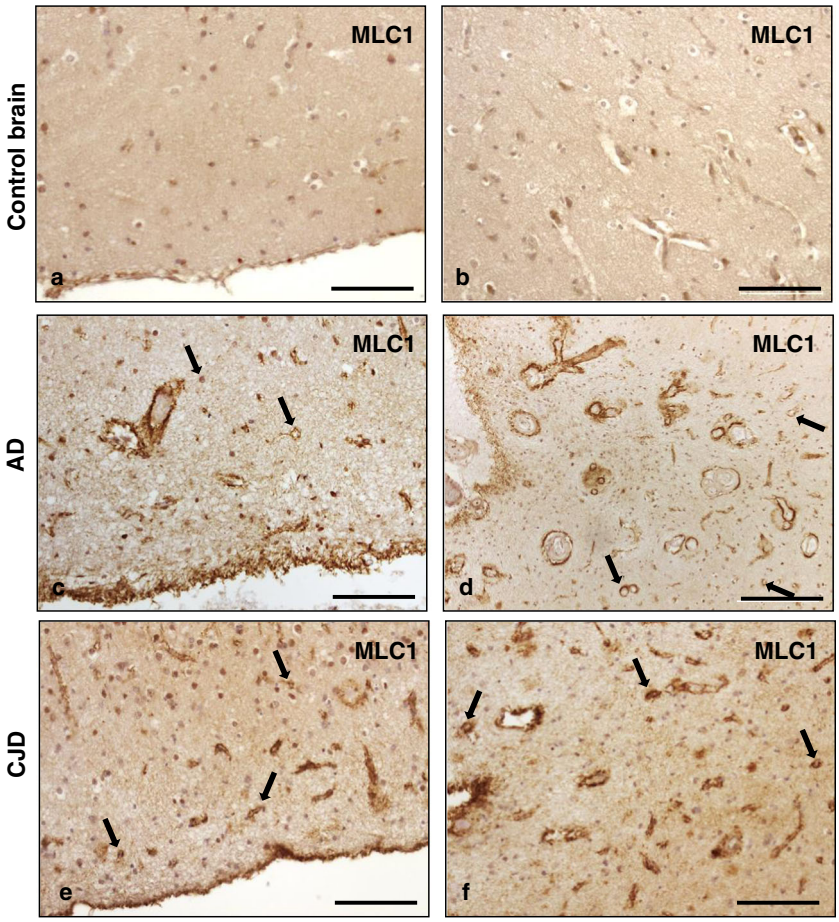

Fig. 2 MLC1 protein expression in tissue from control, Alzheimer's disease (AD) and Creutzfeld-Jacob disease (CJD) brain. Immunohistochemistry for MLC1 was performed on brain sections from one control case (**a**, **b**) and from two donors affected by AD (**c**, **d**) and CJD (**e**, **f**). From each brain section, stainings obtained in subpial gray matter (**a**, **c**, and **e**) and subcortical white matter (**b**, **d**, and **f**) are shown. Compared to control brain where MLC1 was barely detectable in subpial regions (**a**), MLC1 immunoreactivity is strongly increased in the subpial areas and around blood vessels in both AD and CJD brain. Arrows in **c**–**f** point to MLC1-positive small-caliber vessels. Scale bars: 100 μm

we observed MLC1 immunoreactivity in the AD amyloid plaque core (Supplementary Material Fig. 2), where reactive astrocytes have been extensively described [43, 44]. No MLC1 expression was observed in endothelial cells in MS, as previously described [34], (Supplementary Material Fig. 1). The increased expression of MLC1 observed in activated astrocytes in neuroinflammatory diseases, in the absence of blood cell infiltration, suggests that MLC1 protein might be involved in astrocyte activation processes induced by proper neuroinflammatory signals.

The Pro-inflammatory Cytokine IL-1β Favors MLC1 Distribution at Astrocyte Plasma Membrane

To disclose a possible role of MLC1 protein in neuroinflammatory conditions, we investigated the behavior of MLC1 protein in response to astrocyte activation occurring after stimulation with IL-1β, the main inflammatory cytokine released by parenchymal cells in MS, AD, and CJD [45–47]. We first analyzed the consequences of IL-1β treatment on MLC1 expression and localization in the previously characterized U251 human astrocytoma lines overexpressing MLC1 WT or carrying the S280L pathological mutation [23]. We performed preliminary dose response experiments by treating cells with different concentrations of recombinant IL-1β (1, 10, 50 ng/ml) for 12 h (ON). WB analysis revealed that IL-1β induced an increase of the WT MLC1 dimeric component (64 kDa MW form) known to be associated to the cell membrane fraction [32, 34]. This effect was particularly evident after stimulation with 1 and 10 ng/ml of IL-1β, while the highest dose of 50 ng/ml was ineffective (Fig. 4a, b). In the same experiments no statistically significant differences of the S280L mutant MLC1 in response to cytokine treatments were observed (Fig. 4a, b). To evaluate whether IL-1β favored MLC1 distribution specifically at astrocyte plasma membrane, we performed affinity purification of plasma membrane-associated proteins by biotinylation assays on astrocytoma cells expressing WT or mutated MLC1. These experiments showed the enrichment of the 64 kDa MW form of the WT MLC1, but not of the mutated S280L protein, in the plasma membrane protein eluates in response to IL-1β stimulation, where also higher molecular weight oligomers were seen (Fig. 4c, eluates and arrow, respectively). Immunofluorescence experiments confirmed the IL-1β–mediated increase of WT MLC1 at plasma membrane compartment (Fig. 4d–f) and, by contrast, showed the cytoplasmic distribution of

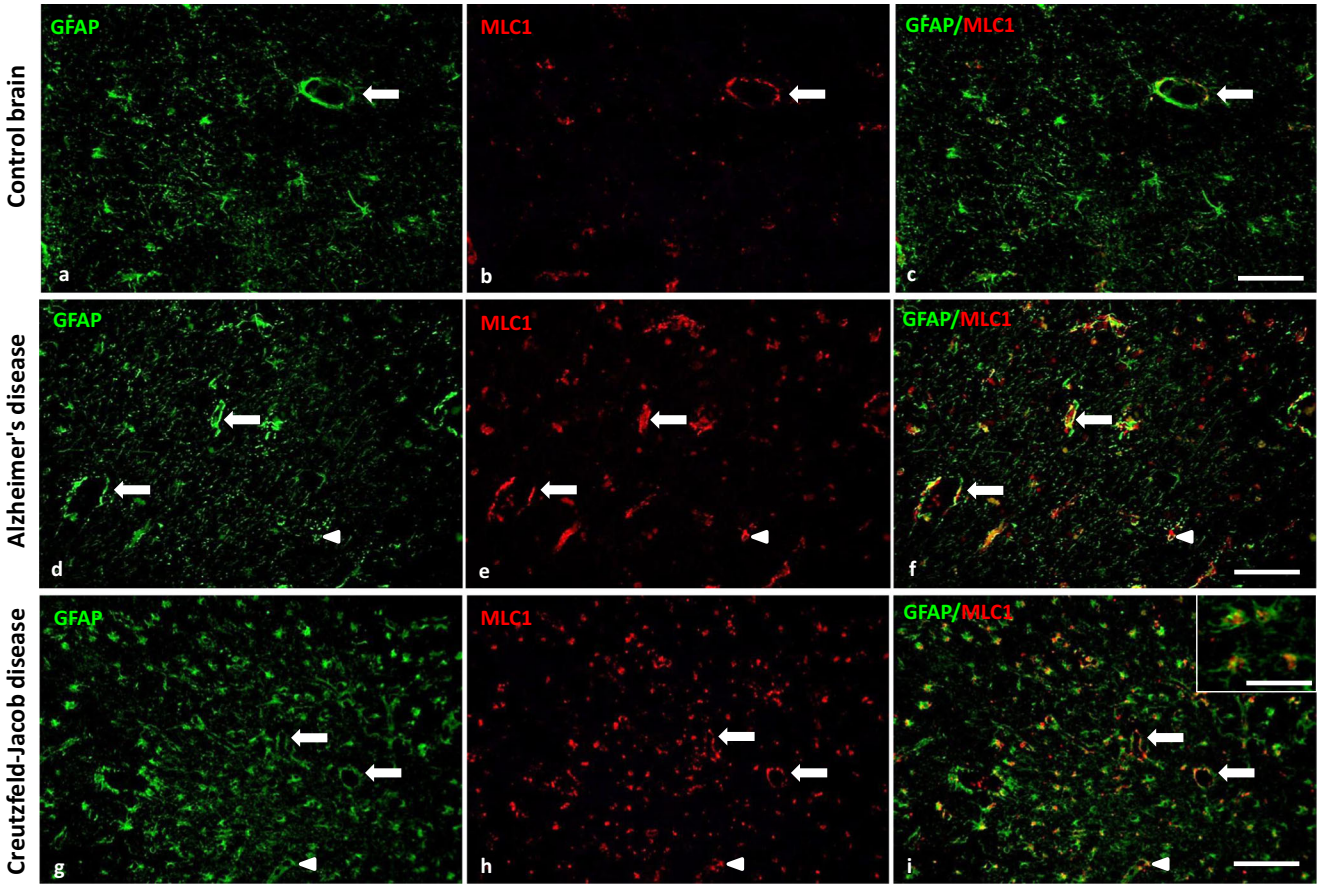

Fig. 3 MLC1 protein expression in brain astrocytes from Control, Alzheimer's (AD), and Creutzfeld-Jacob disease (CJD) tissue samples. Double immunofluorescence stainings for glial fibrillary astrocyte protein (GFAP, green) and MLC1 (red) in the brain of a donor without neurological disease, (control brain, **a**–**c**), a donor with AD (**d**–**f**) and a donor with CJD (**g**–**i**) reveal an increase of MLC1 protein expression in astrocytes contacting large- and small-caliber blood vessels (arrows and arrowheads, respectively) in WM areas of both AD and CJD brains when compared to control samples. In CJD brain tissue several hypertrophic reactive astrocytes expressing MLC1 have also been detected (inset in i). Bars: 100 μm in **a**–**i**; 50 μm in the inset in **i**

the mutant protein (S280L) with or without cytokine treatment (Fig. 4d, f).

Consistent with these results, we found that the endogenous MLC1 expressed in cultured primary rat astrocytes was upregulated by an ON stimulation with 10 ng/ml of IL-1β (Fig. 5a, b). In the same cells, IL-1β treatment did not affect MLC1 mRNA expression (Fig. 5c), suggesting a possible effect of this cytokine on MLC1 protein trafficking and stabilization at the plasma membrane compartment. Results obtained on primary rat astrocytes excluded that the IL-1β–mediated increase of the MLC1 protein observed in U251 astrocytoma cells was not specifically due to MLC1 recombinant expression in cells of tumoral origin.

Altogether, these findings indicated that in astrocytes, the proinflammatory cytokine IL-1β stimulates MLC1 protein translocation and stabilization at plasma membrane. The dual effect of the low (1–10 ng/ml) and high concentrations (50 ng/ml) of IL-1β on MLC1 protein trafficking could be due to the activation of different conflicting signals whose balance determines the final outcome.

WT but Not Mutated MLC1 Protein Expression Inhibits Specific Astrocyte Activation Pathways in Response to IL-1β

We previously observed that in U251 astrocytoma cells, MLC1 overexpression inhibited the phosphorylation of EGFR and ERK1/2 [23], both components of an intracellular signaling pathway involved in astrocyte activation in response to pathological stress. Since EGFR/ERK phosphorylation is also induced by IL-1β [48–51], we investigated the possible influence of MLC1 on the IL-1β-mediated activation of these signaling molecules. To this aim, mock-infected U251 cells (Ø) and cells expressing WT (WT) or mutated MLC1 (S280L) were cultured in the presence or absence of IL-1β and subjected to WB analysis. In control conditions, the phosphorylation of EGFR (pEGFR), that is constitutively activated in U251 cells, was reduced in WT MLC1^{+} cells when compared to U251 mock-infected cells and cells expressing the S280L mutant (Fig. 6a, b), as previously described [23].

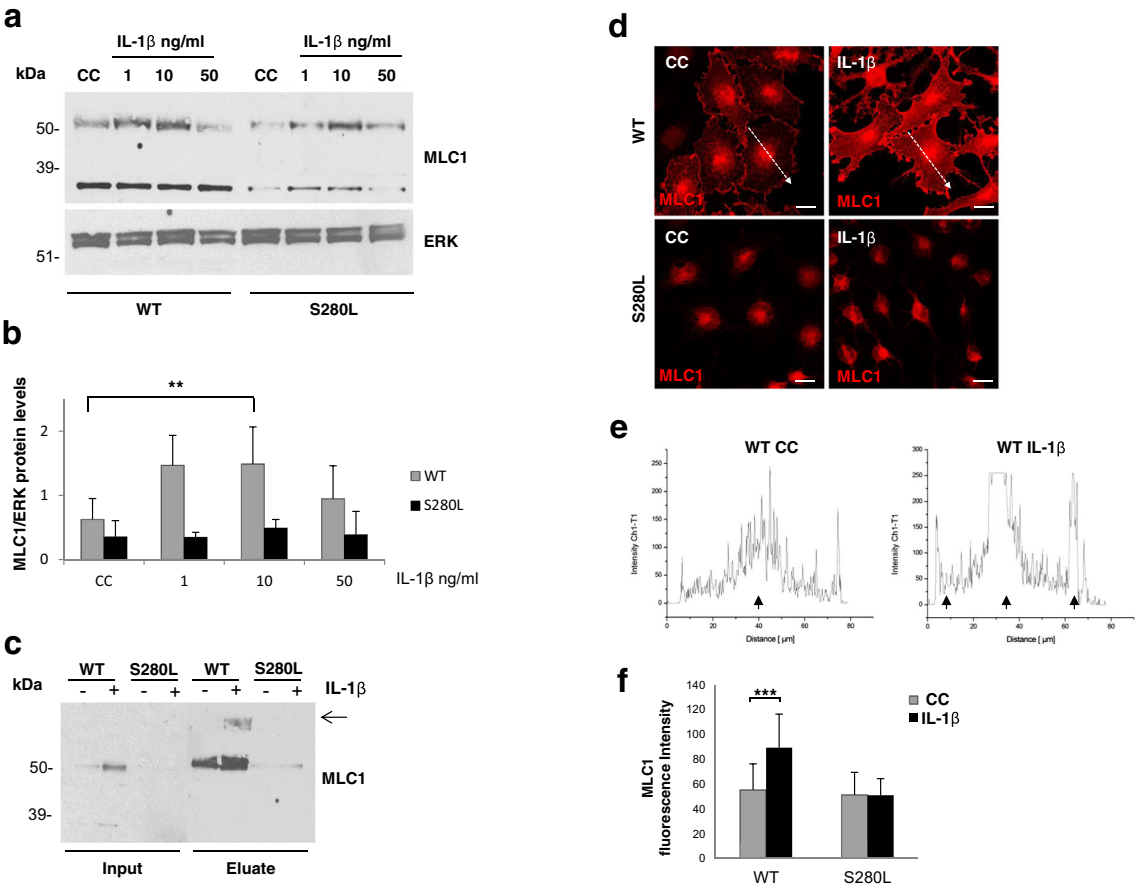

Fig. 4 Effect of interleukin-1 (IL-1β) treatment on MLC1 protein expression in astrocytoma cells. **a** WB analysis of proteins derived from U251 astrocytoma cells expressing WT (WT) or mutated (S280 L) MLC1, untreated (CC) or treated with different concentrations of recombinant IL-1β (1, 10, 50 ng/ml), shows that cytokine treatment induces a significant increase of WT MLC1 protein levels at 1 and 10 ng/ml of IL-1β doses. ERK1/2 is used as loading control. Molecular weight markers are indicated on the left (kDa). One representative experiment out of five performed is shown. **b** Densitometric analysis of MLC1 protein bands after normalization with the loading control protein (ERK) was evaluated in the same samples. The bar graphs represent means ± SEM of five experiments. Significant differences were calculated using Wilcoxon test (**$p < 0.01$). **c** WB of total cell proteins (Input) and of affinity purified plasma membrane proteins (Eluate) from WT and S280L MLC1 cells in control conditions (−) or after IL-1β stimulation (+) shows an increase of the MLC1 dimeric membrane-associated form (64 kDa MW) after IL-1β treatment. The cytoplasmic monomeric MLC1 component (36 kDa MW), used as negative control, is not present in the plasma membrane eluates. High molecular weight oligomers of MLC1 protein are also seen in the plasma membrane eluates (arrow). Molecular weight markers are indicated on the left (kDa). **d** Immunostaining of control (CC) and IL-1β–treated (10 ng/ml) astrocytoma cells overexpressing WT or S280L MLC1 using anti-MLC1 pAb (red) shows an increase in the membrane expression of WT, but not of S280L mutant MLC1 in response to cytokine stimulation. Scale bars: 20 μm. **e** The distribution of immunofluorescence pixel intensity along a freely defined line (dotted arrow in d) spanning the whole cell (plasma membrane-cytoplasm-plasma membrane) was also evaluated using the profile analysis tool of the LSM 5 PASCAL. After IL-1β treatment, MLC1 fluorescence intensity peaks re-distribute from the central perinuclear area, typically observed in control conditions, to a more peripheral cytoplasmic localization and toward the plasma membrane (arrows). **f** The bar graph shows the mean ± SEM values of the MLC1 fluorescence intensity analyzed by the NIH ImageJ software within a region of interest corresponding to a single-cell profile in the astrocytoma cell lines; 10 to 15 random fields (field area = 230 μm^2) were analyzed. Significant differences between CC and IL-1β treated WT MLC1 expressing cells were calculated using Student's *t* test (***$p < 0.001$)

After IL-1β stimulation (10 ng/ml, ON), a slight increase of pEGFR was observed in WT MLC1 cells, while no significant changes were found in mock-infected and S280L mutant expressing cells (Fig. 6a, c). When ERK1/2 activation was monitored, we confirmed that WT MLC1 cells expressed lower levels of pERK when compared to mock-infected and mutant cells in control conditions (Fig. 6a, d). Moreover, IL-1β treatment (10 ng/ml) caused a further reduction of pERK1/2 in WT MLC1 cells, while it did not significantly affect ERK1/2 phosphorylation in mock-infected cells and in cells expressing the MLC1 mutant protein (Fig. 6a, d).

In the same cell populations, we also verified the phosphorylation state of the nuclear factor kappa B (NF-kB), a downstream mediator of IL-1β activated pathways [52], finding that, while in control conditions pNF-kB levels were similar in WT and S280L MLC1 expressing cells, IL-1β stimulation caused a decrease of pNF-kB in WT but not in MLC1 mutant cells (Fig.

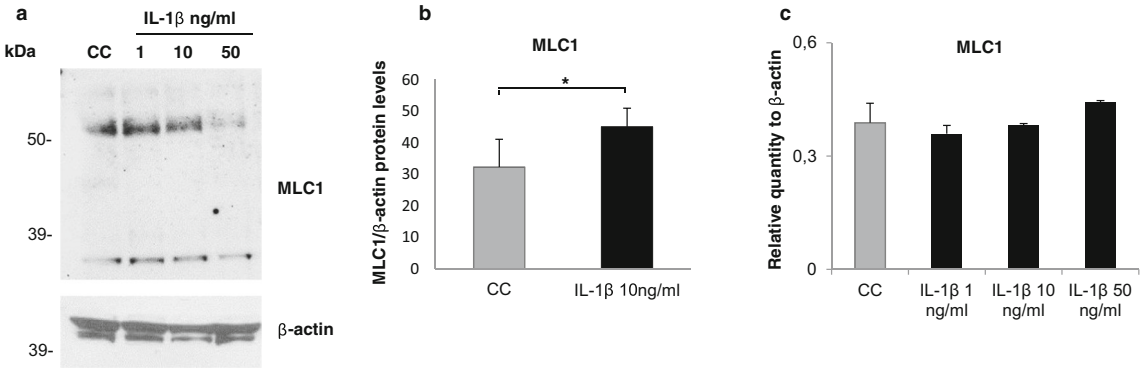

Fig. 5 Effect of IL-1β treatment on MLC1 expression in rat astrocytes. **a** WB analysis of protein extracts derived from primary rat astrocytes, untreated (CC) or treated ON with 1, 10, and 50 ng/ml doses of IL-1β shows MLC1 protein upregulation in response to IL-1β 1 and 10 ng/ml. β-actin is used as loading control. Molecular weight markers are indicated on the left (kDa). One representative experiment out of three performed is shown. **b** Densitometric analysis of MLC1 protein bands revealed by WB after normalization with β-actin protein levels in the same samples. The bar graphs represent means ± SEM of three experiments. Significant differences were calculated using Wilcoxon test (*$p < 0.05$). **c** MLC1 RNA expression was analyzed by real time RT-PCR in control (CC) and IL-1β–treated cells (1, 10, and 50 ng/ml). Results show no difference in MLC1 mRNA levels. RNA levels were normalized using β-actin as reference gene. Bars represent mean ± SEM of three independent experiments

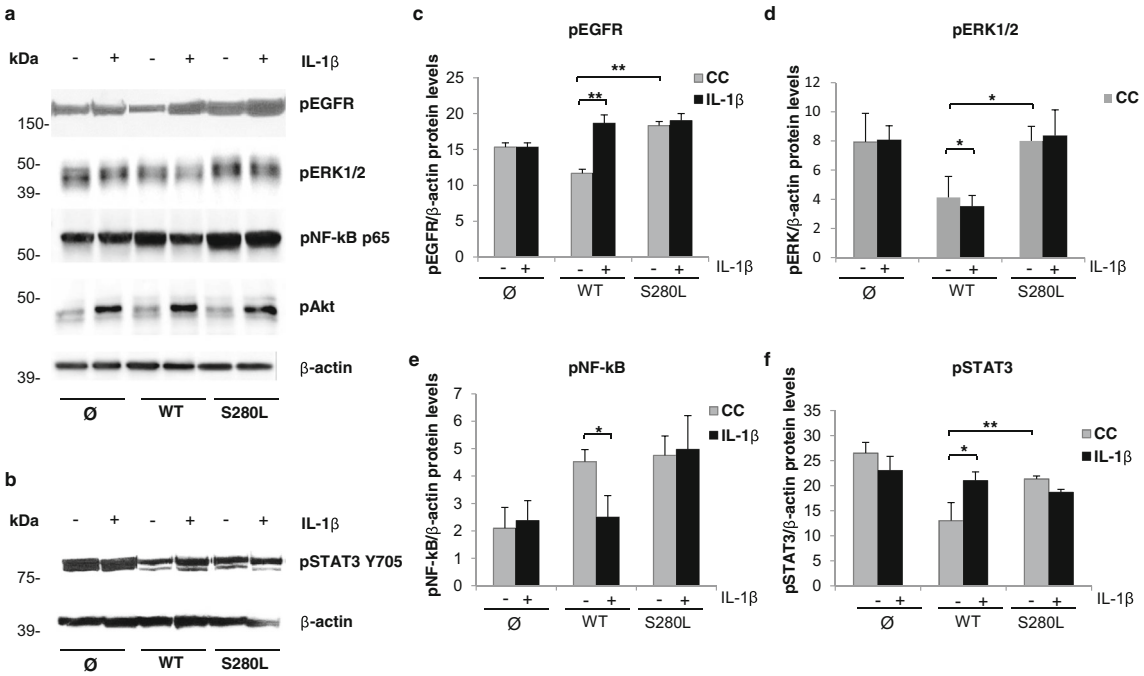

Fig. 6 WT MLC1 influences the phosphorylation of EGFR, ERK1/2, NF-kB, and STAT3 in human astrocytoma cells. **a**, **b** WB analysis of protein extracts from mock-infected U251 cells (Ø), U251 cells expressing MLC1 WT (WT) or carrying the S280L mutation (S280 L). **a** In control condition (−) WT MLC1 cells express lower levels of pEGFR when compared to Ø and S280L cells. Treatment (+) with 10 ng/ml of IL-1β (ON) induces a low level of EGFR phosphorylation in WT MLC1 cells, while no changes are observed in Ø and MLC1 mutant expressing cells (S280L). Reduced amount of pERK1/2 is detected in WT MLC1 when compared to Ø and S280L cells, in control condition (−). IL-1β treatment (+) causes a further reduction of pERK1/2 in WT cells, while it does not affect ERK1/2 phosphorylation in Ø and S280L cells. In control condition (−) pNF-kB levels are similar in WT and S280L cell lines, while a lower amount of pNK-kB is detected in Ø cells. IL-1β treatment (+) leads to a decrease of pNF-kB in WT MLC1 cells, while no changes are observed in the other two cell populations (Ø, S280L). AKT phosphorylation is similar in all the cell lines analyzed. β-actin is used as loading control. **b** In control condition (−), WT MLC1 cells express lower levels of pSTAT3 when compared to Ø, S280L cell lines. IL-1β treatment (1 ng/ml, ON) induces an increase in pSTAT3 expression in WT MLC1 cells while no differences are observed in Ø and S280L cell lines (+). β-actin is used as loading control. Molecular weight markers are indicated on the left (kDa). **c**–**f** Densitometric analysis of pEGFR, pERK1/2, pNF-kB, and pSTAT3 protein bands after β-actin normalization in the same samples is shown. Means ± SEM of five experiments (pEGFR, pERK1/2, pNF-kB) and three experiments (pSTAT3) are shown. Significant differences are calculated using Kruskal-Wallis test followed by Dunn's Multiple Comparison post hoc test. (*$p < 0.05$; **$p < 0.01$)

6a, e). Similarly, in mock-infected cells, whose pNF-kB expression was overall lower than the other two cell lines, cytokine treatment did not change NF-kB activation levels (Fig. 6a, e). To further investigate whether MLC1 protein expression could induce a reactive phenotype in astrocytes, we analyzed the expression/activation of the signal transducer and activator of transcription factor-3 (STAT3), a master regulator of astrocyte reactivity in astrocytes in vivo and in vitro [7, 53, 54] that is constitutively activated in the U251 cell line [55, 56]. Similarly to what described for pEGFR, WB analysis using anti-pSTAT3 Y705 Ab revealed that, in unstimulated conditions, WT MLC1 cells expressed lower levels of pSTAT3 than the mock-infected and mutated cell lines. Increase of pSTAT3 levels were found in WT MLC1 cells after IL1-β stimulation (1 ng/ml), while no changes were observed in the other two cell populations (Ø and S280L), (Fig. 6b, f). No differences were detected in AKT phosphorylation among all the cell lines analyzed (Fig. 6a).

Overall, these data suggested that astrocytoma cells expressing WT MLC1 have a less reactive phenotype than mock-infected and S280L MLC1$^+$ cells. Indeed, cells expressing WT MLC1 showed reduced phosphorylation of most of the signaling molecules analyzed (pEGFR, pERK, pSTAT3), when compared to mock-infected and MLC1 mutant expressing cells, already in basal conditions. Moreover, in WT MLC1$^+$ cells, a further reduction of pERK and pNF-kB was observed after IL-1β stimulation, indicating that MLC1 protein specifically downregulates IL-1β–mediated activation of these two molecules.

Lack of MLC1 in Primary Astrocytes Affects EGFR/ERK and NF-kB Activation

To further study the role of MLC1 in the modulation of signaling pathways associated to astrocyte activation, we extended our studies to the analysis of primary astrocytes derived from wild-type (wt) or *Mlc1* KO mice. Contrary to what was observed in astrocytoma cells overexpressing WT MLC1, WB analysis of mouse cells in unstimulated conditions, showed increased levels of EGFR and ERK1/2 phosphorylation in *Mlc1* KO astrocytes when compared to control ones (Fig. 7a). These results validated the involvement of MLC1 in the modulation of this signaling pathway also in not tumoral astrocytes. We then assessed the consequences of IL-1β stimulation on MLC1 expression in wt mouse astrocytes, finding that, also in these cells, IL-1β (10 ng/ml; ON) stimulated an increase of the endogenous MLC1 protein (Fig. 7b). Similarly, pEGFR, pERK1/2, and pNF-kB levels increased in response to IL-1β stimulation (Fig. 7b–e) in wt astrocytes. By contrast, *Mlc1* KO astrocytes expressed higher levels of pEGFR, pERK1/2, and pNF-kB than wt astrocytes, already in basal conditions, without further significant enhancement after cytokine treatment (Fig. 7b–e). When pSTAT3 expression was evaluated in the same cells, we observed that its activation was extremely variable and dependent on astrocyte maturation stage and cell culture density (data not shown). This variability did not allow us to clearly define the effects of MLC1 lack on STAT3 activation in this cell model.

Altogether, results obtained on primary mouse astrocytes suggested that *Mlc1* KO have a more reactive phenotype than wild-type astrocytes and that the absence of MLC1 protein by itself activates cell reactivity that is not further exacerbated when IL-1β is added.

Analysis of MLC1 Expression Timing in a Demyelinating/Remyelinating Organotypic Brain Slice Model

Data obtained so far revealed that MLC1 protein increases in response to inflammatory signals and that it down-regulates signaling pathways involved in astrocytosis and neuroinflammation. These results led us to hypothesize a possible involvement of MLC1 in restoring astrocyte homeostasis after a pathological activation. To evaluate MLC1 protein behavior during the recovery processes following a brain damage, we monitored MLC1 expression timing in mouse demyelinating/remyelinating organotypic cerebellar slice cultures, in which a toxin-induced demyelination and release of pro-inflammatory cytokines, among which IL-1β, is followed by a spontaneous, partial remyelination [35, 57, 58]. Mouse cerebellar slices grown in culture medium for 7 days were treated with lysolecithin (0.5 mg/ml) to induce demyelination. After 16 h the medium was changed and slices were left in culture to allow axon remyelination. To monitor M*lc1* gene expression, slices were collected immediately after toxin removal (0 h) and after 2 and 4 days in culture and then analyzed by real-time RT-PCR. Figure 8 shows that the expression of MLC1 mRNA was slightly reduced at time 0 h when compared to non-demyelinated control slices, and became significantly higher than control slices at 4 days. These findings revealed that MLC1 expression increases during slice remyelination phase, when tissue homeostasis restoration processes are activated.

To verify whether in the organotypic culture model MLC1 mRNA expression is followed by functional protein production, we also performed WB analysis of cerebellar slices in unstimulated conditions or after hyposmotic treatment that leads to increased MLC1 protein expression and functional activation in astrocytes and patient-derived lymphocytes [16, 59]. Cerebellar slices from P10 mice cultured for 7 days in control medium were stimulated ON with hyposmotic solution and collected for WB analysis. As shown in Supplementary Fig. 3, MLC1 protein expression increased in slices treated with the hyposmotic solution when compared to control ones, indicating that in this experimental ex vivo model, MLC1 retains its functional features.

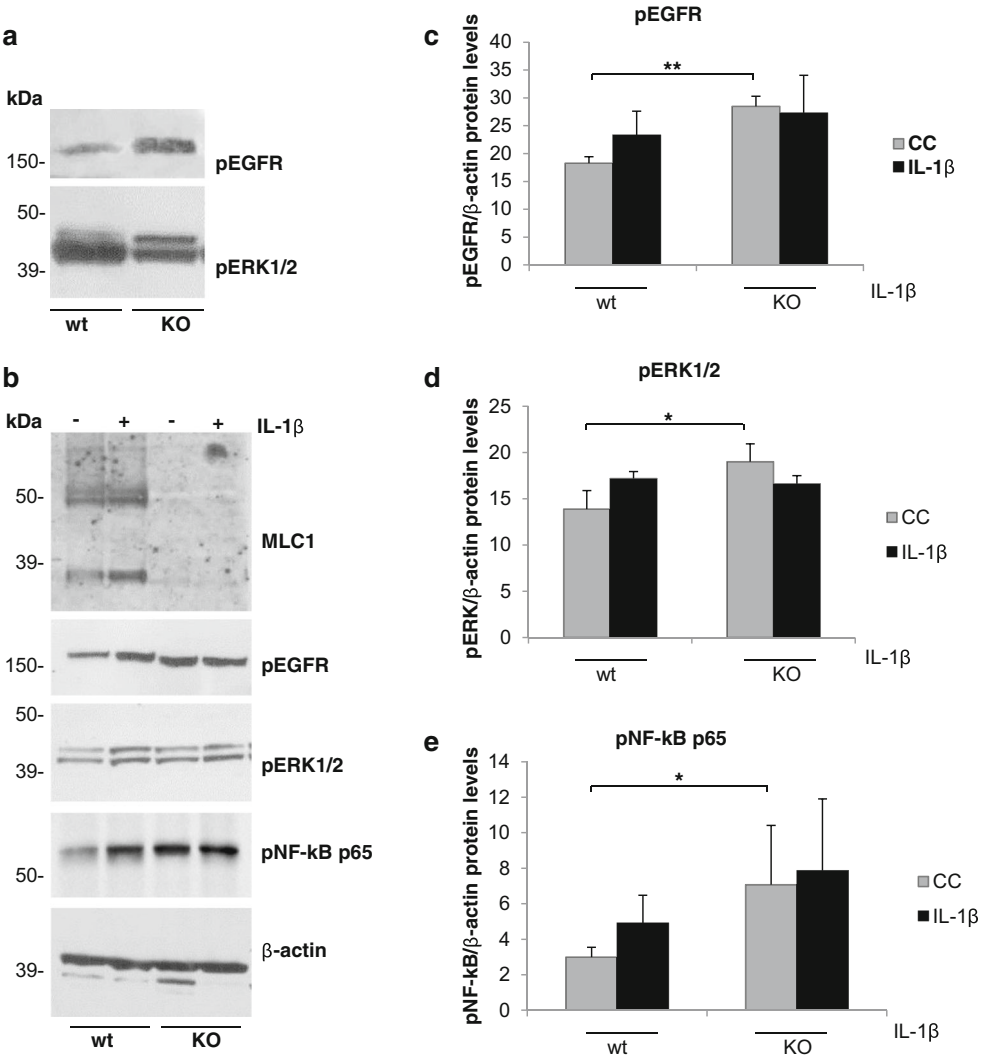

Fig. 7 Analysis of EGFR, ERK1/2, and NF-kB phosphorylation in primary astrocytes from wild-type and *Mlc1* knockout mice. **a** WB analysis of protein extracts from wild-type (wt)- and *Mlc1* knockout (KO)-mouse astrocytes reveals an increase of EGFR and ERK1/2 phosphorylation in KO as compared to wt cells. **b** WB of total protein extracts from wt or *Mlc1* KO astrocytes, untreated (−) and treated (+) with IL-1β (10 ng/ml, ON), indicates that MLC1, pEGFR, pERK1/2, and pNF-kB are upregulated in response to IL-1β stimulation in wt astrocytes. When compared to wt cells, *MLC1* KO astrocytes show higher levels of pEGFR, pERK1/2 and pNF-kB in basal, untreated conditions (−), without further increase after IL-1β treatment (+). β-actin is used as loading control. Molecular weight markers (kDa) are indicated on the left side of panels. **c–e** Densitometric analysis of pEGFR, pERK1/2, pNF-kB protein bands after β-actin normalization in the same samples is shown. The bar graphs represent means ± SEM of four experiments. Significant differences were calculated using Kruskal-Wallis test followed by Dunn's Multiple Comparison post hoc test (*$p < 0.05$; **$p < 0.01$)

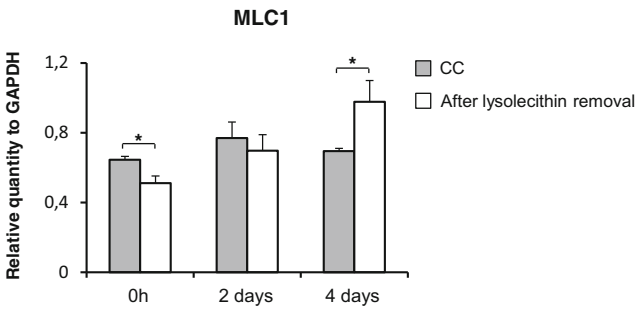

Fig. 8 Regulation of MLC1 transcript during demyelination and remyelination in mouse cerebellar slices. MLC1 RNA expression was analyzed by real time RT-PCR (qPCR) in untreated cerebellar slices (CC) and in lysolecithin-treated slices collected immediately (0 h) and at days 2 and 4 after toxin removal. Results indicate that MLC1 transcript is downregulated in demyelinated slices compared to control at time 0 (0 h), while its expression significantly increases during the remyelination phase (4 days). Data are expressed as $2^{-\Delta Ct}$ relative to GAPDH. Means ± SEM of three experiments are shown. * $p < 0.05$ by Student's *t* test

Discussion

Leukodystrophies are heritable, highly disabling myelin disorders affecting the white matter (WM) of the central nervous system (CNS) and causing cognitive and motor dysfunctions, often leading to severe impairment of vital functions. Dysfunction of glial cells involved in myelin formation and maintenance is the common trait of these diseases. Among leukodystrophies, MLC is caused in 80% of patients by mutations in MLC1, an astrocyte-specific protein whose function is still unknown. Reactive astrocytosis observed in MLC brain and aggravation of patient symptoms after fever or mild trauma [14, 21, 22] suggest that astrocytes abnormally react to changes of brain homeostasis when MLC1 is mutated. The present work was aimed at evaluating the possible involvement of the MLC1 protein in the processes controlling astrocyte activation during neuroinflammation, a pathological condition often occurring after trauma and fever that can lead

MLC patient to coma. Recent findings demonstrating MLC1 involvement in the modulation of intracellular pathways responsible for reactive astrocytosis [23] provided us a conceptual basis to investigate MLC1 function in these processes. Here, by using brain tissue samples from patients affected by neurodegenerative diseases with a strong neuroinflammatory component, cell culture models of MLC and a demyelinating/remyelinating organotypic slice system, we have accumulated evidences indicating that MLC1 protein reacts to inflammatory stimuli by downregulating some intracellular signaling cascades involved in astrocyte activation.

An inflammatory response can be activated following different types of brain insults, including acute trauma, infection, and chronic neurodegenerative diseases [60]. In trauma and infection, circulating bone marrow–derived leukocytes are mainly responsible for the initiation and propagation of the inflammatory response. In chronic neurodegenerative diseases, the inflammatory process is thought to originate primarily from CNS cells. Coordinated interactions among glial cells (particularly microglia and astrocytes) are required for the fine-tuned regulation and resolution of the inflammatory response, preservation of healthy tissue, and restriction of inflammation spread [4].

We and others previously reported increased MLC1 expression in brain tissue from patients affected by multiple sclerosis (MS), the paradigmatic inflammatory disease of the CNS, where a strong upregulation of MLC1 was found in areas of active demyelination and inflammatory cell infiltration [38, 59]. In the present paper we further extended our analysis by evaluating MLC1 expression in not demyelinated MS brain areas characterized by the presence of activated microglial cells, without inflammatory blood cell extravasation, and in normal appearing white matter (NAWM), where only scattered activated microglial cells are present. Our results highlighted MLC1 upregulation in these not demyelinated areas, particularly in astrocyte contacting blood vessels, but also in several parenchymal, hypertrophic astrocytes in close proximities to activated microglia, suggesting that MLC1 protein expression is stimulated by inflammatory signals, most likely released by parenchymal cells. Similarly, increased MLC1 protein expression in perivascular astrocytes was also found in brain tissue from patients affected by other neurodegenerative diseases, such as Alzheimer's (AD) and Creutzfeld-Jacob (CJD) that are both characterized by strong astrocytosis and release of inflammatory mediators. Indeed, in CJD and AD, amyloid formation leads to a neuroinflammatory response [61–64] with secondary neurofibrillary degeneration [65] and persistent activation of microglia and astrocytes [66–68]. In these diseases, astrocytes are emerging as important contributors to the pathological mechanism [69, 70]. Reactive astrocytes have been described in the brain of AD and CJD patients where inflammation occurs due to the release by activated glia of a number of potentially toxic molecules, including pro-inflammatory chemokines and cytokines [46, 69–72]. Here, we observed MLC1 protein expression in typical hypertrophic astrocytes characterizing CJD brain tissue and in amyloid plaques in AD samples where astrocyte reactivity has been described to progress in parallel to amyloid pathology [43, 44]. Whether MLC1 contributes to amyloid plaque formation or is the result of the interaction between astrocytes and plaques at an advanced stage of the disease has yet to be determined. Altogether, these neuropathological findings indicate that MLC1 might play a role during astrocyte activation in a proper neuroinflammatory context.

We then explored the effect of IL-1β treatment on MLC cellular models. IL-1β produced by microglial cells is the main inflammatory cytokine released during neuroinflammation in MS, AD, and CJD [45–47]. An increased concentration of IL-1β was also found in brain after trauma [73] and fever [74], two pathological conditions causing extremely severe consequences for MLC patients. Interestingly, in the animal model of these latter diseases, pharmacological inhibition of IL-1β favors resolution of inflammation and decrease of edema [75, 76] that is one of the most typical pathological consequences of MLC. Our results revealed that IL-1β promotes WT MLC1 translocation and stabilization at plasma membranes in all the different types of astrocytes analyzed (human astrocytoma cells and primary rat and mouse astrocytes), suggesting that the inflammatory environment specifically induced by IL-1β can stimulate MLC1 function. In vivo and in vitro experiments demonstrated that in glial cells IL-1β activates MAPK-ERK intracellular pathway [48, 49, 51, 77, 78] that we previously found inhibited by MLC1 in astrocytoma cells [23]. To study the possible involvement of MLC1 in the control of signaling pathways activated during inflammatory processes in astrocytes, we took advantages by the use of two different MLC cellular models: *i)* U251 human astrocytoma cells overexpressing WT or mutated (S280L) MLC1 and *ii)* primary mouse astrocytes from control and *Mlc1* KO mice. Results obtained in these experiments indicated that MLC1 overexpression, by reducing the constitutive activation of pEGFR, pERK1/2, pSTAT3, and the IL-1β–mediated activation of pERK and pNF-kB in the astrocytoma cells could affect astrocyte activation during inflammatory processes. Consistent with this hypothesis, we observed that lack of MLC1 in primary mouse astrocytes caused the abnormal activation of pEGFR, pERK1/2, and pNF-kB, also in absence of inflammatory stimulation, confirming the down-modulatory role of MLC1 on these astrocyte- activation pathways. Within this scenario, it is conceivable that dysfunctional MLC1 can provoke abnormal and/or prolonged astrocyte activation in response to pathological stimulation in MLC patients. Mitogen-activated protein kinases (MAPKs), including ERK kinases, are a family of serine/threonine protein kinases responsible for most cellular responses to cytokines and external stress signals and contribute to the pathogenesis of several

neurodegenerative, neuroinflammatory, and developmental diseases [79, 80]. Noteworthy, peripheral administration of IL-1β in rat has been demonstrated to activate the phosphorylation of ERK1/2 in vivo in areas at the interface between brain and blood or cerebrospinal fluid [49], where MLC1 is mainly expressed in the CNS. In addition, experimental in vitro and in vivo evidences indicated that IL-1β causes astrocyte swelling via NF-kB activation [81] and brain edema following different types of injuries [75] and that inhibition of ERK kinases can favor edema resolution [82–84]. All these evidences reinforce our hypothesis of a possible pathophysiological role of MLC1 in down-modulating the astrocytic response to inflammatory signals, such as the IL-1β–mediated activation of pERK and pNF-kB. The abnormal or persistent activation of these molecules may account for astrocyte swelling (Fig. 9), particularly at BBB, where swelled, vacuolated astrocytes were observed in MLC brain tissues [85]. Astrocyte swelling is one of the hallmarks of reactive astrogliosis and it occurs in response to inflammation during ischemia and brain trauma [18, 75, 86, 87]. Astrocytes can counteract these deleterious volume increases with the extrusion of Cl^- and K^+ and osmotically water, leading to regulatory volume decrease (RVD), the physiological process regulated by MLC1 [16]. It is conceivable that, by acting on specific signaling pathways, MLC1 favors the activation of RVD, thus reducing astrocyte swelling and reactive astrogliosis.

Accordingly, we observed a decrease of the reactive astrocytosis marker pSTAT3 in astrocytoma cells overexpressing WT MLC1. These results are particularly relevant since the JAK2-STAT3 pathway is a master regulator of astrocyte reactivity in vivo, by favoring the induction and long-term maintenance of reactive astrocytes [88]. Although, we were not able to study pSTAT3 behavior in primary astrocytes derived from wt or *Mlc1* KO mice because of the extreme sensitivity of this factor to cell culture conditions (i.e., astrocyte maturation stage and cellular density), results obtained on the other signaling molecules in the astrocytoma and primary astrocyte models revealed that cells deprived of MLC1 have a more reactive phenotype than WT-MLC1 expressing cells.

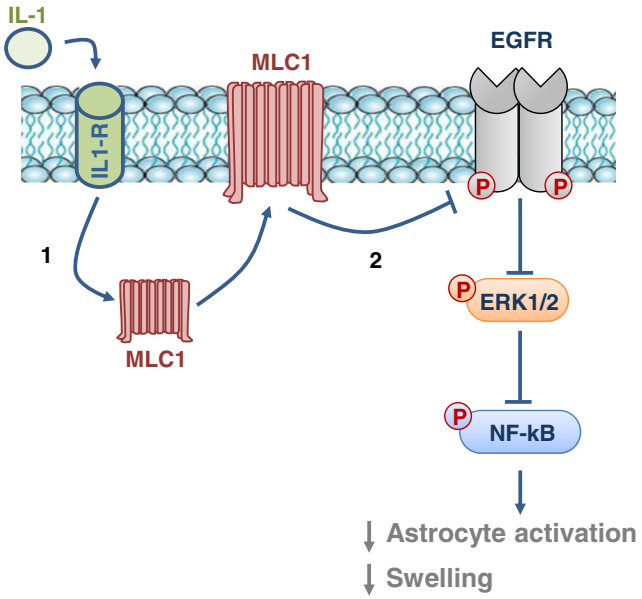

Fig. 9 Schematic representation of MLC1 regulation on IL1-β–mediated intracellular signaling pathway activation in astrocytes. (1) IL-1β stimulation increases MLC1 protein translocation at astrocyte plasma membrane. (2) Functionally active MLC1, stabilized at plasma membrane, inhibits IL-1β–mediated activation of pERK/pNF-kB, leading to down-regulation of astrocyte activation and swelling

While a moderate astrogliosis seems essential in the recovery of injured CNS since it stimulates astrocyte release of neurotrophic factors, a severe and prolonged process can cause a strong inflammatory response that become toxic to neurons, ultimately leading them to death [88]. Prolonged or excessive astrocyte activation can also affect myelin, as observed in Alexander disease and Vanishing White Matter [9], and reference therein], other two rare leukodystrophies caused by primary astrocyte dysfunctions. However, since astrocyte activation is the result of a complex multifactorial and multistage process where coordinated interactions of different cells occurs [1, 4], we cannot exclude that other different intracellular signaling pathways linked to IL-1β or/and other pro-inflammatory mediators released by microglia (or astrocyte themselves) are influenced directly or indirectly by MLC1. The temporal pattern of MLC1 expression observed in cerebellar organotypic cultures, where lysolecithin treatment causes a reversible demyelination and inflammation with increased expression of IL-1β [77], Veroni et al., submitted], revealed that MLC1 expression is upregulated in the tissue remyelination phase, when homeostatic conditions have to be restored. These data support the hypothesis that MLC protein works to re-establish astrocyte homeostasis after their activation in response to damaging signals.

Accordingly, recent studies performed on a transgenic mouse model expressing a MLC1-GFP chimeric protein showed that MLC1 expression is progressively induced in reactive astrocytes forming the glial scar after a stab wound cortical injury [89].

It has also been hypothesized that MLC1 is involved in the spatial buffering of K^+ ions in conditions of high neuronal activity [90, 91]. A recent study aimed at investigating the cellular basis of epilepsy in MLC revealed dysregulation of $[K^+]o$ network, hyperexcitability and seizures in the hippocampus of *Mlc1* KO mice [92]. Acute brain insults and many chronic brain diseases can cause inflammatory response, glia activation, and increased neuronal excitability leading to neuronal depolarization, repetitive firing, and potassium ion release [93]. External K^+ increase is also a consequence of many pathological states in the CNS where swelling and GFAP up-regulation are observed [94]. Altogether, these findings indicate that inflammatory events could cause accumulation of K^+

and consequent cell volume disturbances and seizures in MLC patients.

Overall, our results support the hypothesis that MLC1 is involved in the response of astrocytes to stress/inflammatory stimuli and the underlying pathways, and that defects of this function may account for the clinical features of the disease, such as abnormal and/or prolonged response to inflammatory and traumatic events, seizures, or even demyelination. Indeed, Erk2 activation in astrocytes plays a crucial role in aggravating demyelinating inflammation by inducing inflammatory mediators and gliosis [95]. Thus, therapies blocking Erk2 activation in glial cells could represent a promising approach for the treatment of distinct demyelinating diseases, including MLC. Importantly, the observation that MLC patients carrying dominant mutations in *GlialCAM*, the second gene linked to MLC, show a partial MRI remitting phenotype and improvement of clinical parameters during time [96], indicated that the MLC pathological process is, at least partially, reversible. These findings give hope that the correction of MLC1 mutation-associated dysfunctional pathways may arrest disease progression and ameliorate neurological symptoms. Elucidation of MLC1 protein function in the regulation of astrocyte protective versus detrimental responses could also reveal new potential therapeutic targets for other neuroinflammatory and neurodegenerative diseases.

Acknowledgments We thank Dr. Antonella Bernardo for providing rat astrocyte cultures, Dr. Barbara Rosicarelli for technical assistance in the immunohistochemical work, and the UK Multiple Sclerosis Tissue Bank (http://www.imperial.ac.uk/medicine/multiple-sclerosis-and-parkinsons-tissue-bank) for providing brain tissue samples.

Fundings This work was supported by Italian Ministry of Health, Ricerca Finalizzata, (Grant N. GR-2013-02355882 to A.L.); European Leukodystrophies Association (ELA) (Grant N. ELA 2016-002F3 to M.S.B and ELA2012-014C2B to R.E.); TELETHON (Grant N. GEP14134 to E.A.); Spanish Ministerio de Ciencia e Innovación (MICINN) (SAF2015–70377 to R.E.); and the Generalitat de Catalunya (SGR2014–1178 to R.E.), (ERARE to R.E.). R.E. is a recipient of an ICREA Academia prize.

Compliance with Ethical Standards

Conflict of Interest The authors declare that they have no conflict of interest.

References

1. Sofroniew MV, Vinters HV (2010) Astrocytes: biology and pathology. Acta Neuropathol 119:7–35
2. Pekny M, Pekna M (2014) Astrocyte reactivity and reactive astrogliosis: costs and benefits. Physiol Rev 94:1077–1098
3. Pekny M, Wilhelmsson U, Pekna M (2014) The dual role of astrocyte activation and reactive gliosis. Neurosci Lett 565:30–38
4. Liddelow SA, Barres BA (2017) Reactive astrocytes: production, function, and therapeutic potential. Immunity. 46:957–967
5. Pekny M, Pekna M (2016) Reactive gliosis in the pathogenesis of CNS diseases. Biochim Biophys Acta 1862:483–491
6. Pekny M, Pekna M, Messing A, Steinhauser C, Lee JM, Parpura V, Hol EM, Sofroniew MV et al (2016) Astrocytes: a central element in neurological diseases. Acta Neuropathol 131:323–345
7. Ben Haim L, Carrillo-de Sauvage MA, Ceyzeriat K, Escartin C (2015) Elusive roles for reactive astrocytes in neurodegenerative diseases. Front Cell Neurosci 9:278
8. Ferrer I (2017) Diversity of astroglial responses across human neurodegenerative disorders and brain aging. Brain Pathol 27:645–674
9. Lanciotti A, Brignone MS, Bertini E, Petrucci TC, Aloisi F, Ambrosini E (2013) Astrocytes: emerging stars in leukodystrophy pathogenesis. Transl Neurosci 4. https://doi.org/10.2478/s13380-013-0118-1
10. Leegwater PA, Boor PK, Yuan BQ, van der Steen J, Visser A, Konst AA, Oudejans CB, Schutgens RB et al (2002) Identification of novel mutations in MLC1 responsible for megalencephalic leukoencephalopathy with subcortical cysts. Hum Genet 110:279–283
11. Leegwater PA, Yuan BQ, van der Steen J, Mulders J, Konst AA, Boor PK, Mejaski-Bosnjak V, van der Maarel SM et al (2001) Mutations of MLC1 (KIAA0027), encoding a putative membrane protein, cause megalencephalic leukoencephalopathy with subcortical cysts. Am J Hum Genet 68:831–838
12. Yalcinkaya C, Yuksel A, Comu S, Kilic G, Cokar O, Dervent A (2003) Epilepsy in vacuolating megalencephalic leukoencephalopathy with subcortical cysts. Seizure. 12:388–396
13. van der Knaap MS, Barth PG, Vrensen GF, Valk J (1996) Histopathology of an infantile-onset spongiform leukoencephalopathy with a discrepantly mild clinical course. Acta Neuropathol 92:206–212
14. Pascual-Castroviejo I, van der Knaap MS, Pronk JC, Garcia-Segura JM, Gutierrez-Molina M, Pascual-Pascual SI (2005) Vacuolating megalencephalic leukoencephalopathy: 24 year follow-up of two siblings. Neurologia. 20:33–40
15. Duarri A, Lopez de Heredia M, Capdevila-Nortes X, Ridder MC, Montolio M, Lopez-Hernandez T, Boor I, Lien CF et al (2011) Knockdown of MLC1 in primary astrocytes causes cell vacuolation: a MLC disease cell model. Neurobiol Dis 43:228–238
16. Ridder MC, Boor I, Lodder JC, Postma NL, Capdevila-Nortes X, Duarri A, Brussaard AB, Estevez R et al (2011) Megalencephalic leucoencephalopathy with cysts: defect in chloride currents and cell volume regulation. Brain. 134:3342–3354
17. Dubey M, Bugiani M, Ridder MC, Postma NL, Brouwers E, Polder E, Jacobs JG, Baayen JC et al (2015) Mice with megalencephalic leukoencephalopathy with cysts: a developmental angle. Ann Neurol 77:114–131
18. Jayakumar AR, Rao KV, Panickar KS, Moriyama M, Reddy PV, Norenberg MD (2008) Trauma-induced cell swelling in cultured astrocytes. J Neuropathol Exp Neurol 67:417–427
19. Pasantes-Morales H, Vazquez-Juarez E (2012) Transporters and channels in cytotoxic astrocyte swelling. Neurochem Res 37:2379–2387
20. Brosnan CF, Raine CS (2013) The astrocyte in multiple sclerosis revisited. Glia. 61:453–465
21. Bugiani M, Moroni I, Bizzi A, Nardocci N, Bettecken T, Gartner J, Uziel G (2003) Consciousness disturbances in megalencephalic leukoencephalopathy with subcortical cysts. Neuropediatrics. 34:211–214
22. Mejaski-Bosnjak V, Besenski N, Brockmann K, Pouwels PJ, Frahm J, Hanefeld FA (1997) Cystic leukoencephalopathy in a megalencephalic child: clinical and magnetic resonance imaging/magnetic resonance spectroscopy findings. Pediatr Neurol 16:347–350
23. Lanciotti A, Brignone MS, Visentin S, De Nuccio C, Catacuzzeno L, Mallozzi C, Petrini S, Caramia M et al (2016) Megalencephalic

leukoencephalopathy with subcortical cysts protein-1 regulates epidermal growth factor receptor signaling in astrocytes. Hum Mol Genet 25:1543–1558
24. Gao WL, Tian F, Zhang SQ, Zhang H, Yin ZS (2014) Epidermal growth factor increases the expression of Nestin in rat reactive astrocytes through the Ras-Raf-ERK pathway. Neurosci Lett 562:54-59
25. Burda JE, Sofroniew MV (2014) Reactive gliosis and the multicellular response to CNS damage and disease. Neuron. 81:229–248
26. Wei T, Yi M, Gu W, Hou L, Lu Q, Yu Z, Chen H (2017) The Potassium Channel KCa3.1 represents a valid pharmacological target for Astrogliosis-induced neuronal impairment in a mouse model of Alzheimer's disease. Front Pharmacol 7:528
27. Yi M, Wei T, Wang Y, Lu Q, Chen G, Gao X, Geller HM, Chen H et al (2017) The potassium channel KCa3.1 constitutes a pharmacological target for astrogliosis associated with ischemia stroke. J Neuroinflammation 14:203–017-0973-8
28. Elorza-Vidal X, Sirisi S, Gaitan-Penas H, Perez-Rius C, Alonso-Gardon M, Armand-Ugon M, Lanciotti A, Brignone MS et al (2018) GlialCAM/MLC1 modulates LRRC8/VRAC currents in an indirect manner: implications for megalencephalic leukoencephalopathy. Neurobiol Dis 119:88–99
29. Petrini S, Minnone G, Coccetti M, Frank C, Aiello C, Cutarelli A, Ambrosini E, Lanciotti A et al (2013) Monocytes and macrophages as biomarkers for the diagnosis of megalencephalic leukoencephalopathy with subcortical cysts. Mol Cell Neurosci 56:307–321
30. Agresti C, Aloisi F, Levi G (1991) Heterotypic and homotypic cellular interactions influencing the growth and differentiation of bipotential oligodendrocyte-type-2 astrocyte progenitors in culture. Dev Biol 144:16–29
31. Lanciotti A, Brignone MS, Molinari P, Visentin S, De Nuccio C, Macchia G, Aiello C, Bertini E et al (2012) Megalencephalic leukoencephalopathy with subcortical cysts protein 1 functionally cooperates with the TRPV4 cation channel to activate the response of astrocytes to osmotic stress: dysregulation by pathological mutations. Hum Mol Genet 21:2166–2180
32. Lanciotti A, Brignone MS, Camerini S, Serafini B, Macchia G, Raggi C, Molinari P, Crescenzi M et al (2010) MLC1 trafficking and membrane expression in astrocytes: role of caveolin-1 and phosphorylation. Neurobiol Dis 37:581–595
33. Brignone MS, Lanciotti A, Visentin S, De Nuccio C, Molinari P, Camerini S, Diociaiuti M, Petrini S et al (2014) Megalencephalic leukoencephalopathy with subcortical cysts protein-1 modulates endosomal pH and protein trafficking in astrocytes: relevance to MLC disease pathogenesis. Neurobiol Dis 66:1–18
34. Ambrosini E, Serafini B, Lanciotti A, Tosini F, Scialpi F, Psaila R, Raggi C, Di Girolamo F et al (2008) Biochemical characterization of MLC1 protein in astrocytes and its association with the dystrophin-glycoprotein complex. Mol Cell Neurosci 37:480–493
35. Eleuteri C, Olla S, Veroni C, Umeton R, Mechelli R, Romano S, Buscarinu MC, Ferrari F et al (2017) A staged screening of registered drugs highlights remyelinating drug candidates for clinical trials. Sci Rep 7:45780
36. Lassmann H (2018) Multiple sclerosis pathology. Cold Spring Harb Perspect Med 8. https://doi.org/10.1101/cshperspect.a028936
37. Stadelmann C (2011) Multiple sclerosis as a neurodegenerative disease: pathology, mechanisms and therapeutic implications. Curr Opin Neurol 24:224–229
38. Boor PK, de Groot K, Waisfisz Q, Kamphorst W, Oudejans CB, Powers JM, Pronk JC, Scheper GC et al (2005) MLC1: a novel protein in distal astroglial processes. J Neuropathol Exp Neurol 64:412–419
39. Stephenson J, Nutma E, van der Valk P, Amor S (2018) Inflammation in CNS neurodegenerative diseases. Immunology. 154:204–219
40. Zenaro E, Piacentino G, Constantin G (2017) The blood-brain barrier in Alzheimer's disease. Neurobiol Dis 107:41–56
41. Iwasaki Y, Mori K, Ito M, Tatsumi S, Mimuro M, Yoshida M (2013) An autopsied case of progressive supranuclear palsy presenting with cerebellar ataxia and severe cerebellar involvement. Neuropathology. 33:561–567
42. Lewicki H, Tishon A, Homann D, Mazarguil H, Laval F, Asensio VC, Campbell IL, DeArmond S et al (2003) T cells infiltrate the brain in murine and human transmissible spongiform encephalopathies. J Virol 77:3799–3808
43. Verkhratsky A, Zorec R, Rodriguez JJ, Parpura V (2016) Astroglia dynamics in ageing and Alzheimer's disease. Curr Opin Pharmacol 26:74–79
44. Gomez-Arboledas A, Davila JC, Sanchez-Mejias E, Navarro V, Nunez-Diaz C, Sanchez-Varo R, Sanchez-Mico MV, Trujillo-Estrada L et al (2018) Phagocytic clearance of presynaptic dystrophies by reactive astrocytes in Alzheimer's disease. Glia. 66:637–653
45. Van Everbroeck B, Dewulf E, Pals P, Lubke U, Martin JJ, Cras P (2002) The role of cytokines, astrocytes, microglia and apoptosis in Creutzfeldt-Jakob disease. Neurobiol Aging 23:59–64
46. Rubio-Perez JM, Morillas-Ruiz JM (2012) A review: inflammatory process in Alzheimer's disease, role of cytokines. ScientificWorldJournal. 2012:756357
47. Lucas SM, Rothwell NJ, Gibson RM (2006) The role of inflammation in CNS injury and disease. Br J Pharmacol 147(Suppl 1):S232–S240
48. Parker LC, Luheshi GN, Rothwell NJ, Pinteaux E (2002) IL-1 beta signalling in glial cells in wildtype and IL-1RI deficient mice. Br J Pharmacol 136:312–320
49. Nadjar A, Combe C, Busquet P, Dantzer R, Parnet P (2005) Signaling pathways of interleukin-1 actions in the brain: anatomical distribution of phospho-ERK1/2 in the brain of rat treated systemically with interleukin-1beta. Neuroscience. 134:921–932
50. Meini A, Sticozzi C, Massai L, Palmi M (2008) A nitric oxide/Ca(2+)/calmodulin/ERK1/2 mitogen-activated protein kinase pathway is involved in the mitogenic effect of IL-1beta in human astrocytoma cells. Br J Pharmacol 153:1706–1717
51. Summers L, Kangwantas K, Nguyen L, Kielty C, Pinteaux E (2010) Adhesion to the extracellular matrix is required for interleukin-1 beta actions leading to reactive phenotype in rat astrocytes. Mol Cell Neurosci 44:272–281
52. Marcus JS, Karackattu SL, Fleegal MA, Sumners C (2003) Cytokine-stimulated inducible nitric oxide synthase expression in astroglia: role of Erk mitogen-activated protein kinase and NF-kappaB. Glia. 41:152–160
53. Wang T, Yuan W, Liu Y, Zhang Y, Wang Z, Zhou X, Ning G, Zhang L et al (2015) The role of the JAK-STAT pathway in neural stem cells, neural progenitor cells and reactive astrocytes after spinal cord injury. Biomed Rep 3:141–146
54. Ben Haim L, Ceyzeriat K, Carrillo-de Sauvage MA, Aubry F, Auregan G, Guillermier M, Ruiz M, Petit F et al (2015) The JAK/STAT3 pathway is a common inducer of astrocyte reactivity in Alzheimer's and Huntington's diseases. J Neurosci 35:2817–2829
55. Konnikova L, Kotecki M, Kruger MM, Cochran BH (2003) Knockdown of STAT3 expression by RNAi induces apoptosis in astrocytoma cells. BMC Cancer 3:23–2407-3-23
56. Lindemann C, Hackmann O, Delic S, Schmidt N, Reifenberger G, Riemenschneider MJ (2011) SOCS3 promoter methylation is mutually exclusive to EGFR amplification in gliomas and promotes glioma cell invasion through STAT3 and FAK activation. Acta Neuropathol 122:241–251
57. Barateiro A, Afonso V, Santos G, Cerqueira JJ, Brites D, van Horssen J, Fernandes A (2016) S100B as a potential biomarker

and therapeutic target in multiple sclerosis. Mol Neurobiol 53: 3976–3991
58. Birgbauer E, Rao TS, Webb M (2004) Lysolecithin induces demyelination in vitro in a cerebellar slice culture system. J Neurosci Res 78:157–166
59. Brignone MS, Lanciotti A, Macioce P, Macchia G, Gaetani M, Aloisi F, Petrucci TC, Ambrosini E (2011) The beta1 subunit of the Na,K-ATPase pump interacts with megalencephalic leucoencephalopathy with subcortical cysts protein 1 (MLC1) in brain astrocytes: New insights into MLC pathogenesis. Hum Mol Genet 20:90–103
60. Sofroniew MV (2015) Astrocyte barriers to neurotoxic inflammation. Nat Rev Neurosci 16:249–263
61. Griffin WS (2006) Inflammation and neurodegenerative diseases. Am J Clin Nutr 83:470S–474S
62. Griffin WS, Liu L, Li Y, Mrak RE, Barger SW (2006) Interleukin-1 mediates Alzheimer and Lewy body pathologies. J Neuroinflammation 3:5–2094-3-5
63. Rezaie P, Lantos PL (2001) Microglia and the pathogenesis of spongiform encephalopathies. Brain Res Brain Res Rev 35:55–72
64. Amor S, Peferoen LA, Vogel DY, Breur M, van der Valk P, Baker D, van Noort JM (2014) Inflammation in neurodegenerative diseases–an update. Immunology. 142:151–166
65. Rozemuller AJ, Jansen C, Carrano A, van Haastert ES, Hondius D, van der Vies SM, Hoozemans JJ (2012) Neuroinflammation and common mechanism in Alzheimer's disease and prion amyloidosis: amyloid-associated proteins, neuroinflammation and neurofibrillary degeneration. Neurodegener Dis 10:301–304
66. Heneka MT (2017) Inflammasome activation and innate immunity in Alzheimer's disease. Brain Pathol 27:220–222
67. Guillot-Sestier MV, Town T (2017) Let's make microglia great again in neurodegenerative disorders. J Neural Transm (Vienna)
68. Stoeck K, Schmitz M, Ebert E, Schmidt C, Zerr I (2014) Immune responses in rapidly progressive dementia: a comparative study of neuroinflammatory markers in Creutzfeldt-Jakob disease, Alzheimer's disease and multiple sclerosis. J Neuroinflammation 11:170–014-0170-y
69. Aguzzi A, Liu Y (2017) A role for astroglia in prion diseases. J Exp Med 214:3477–3479
70. Avila-Munoz E, Arias C (2014) When astrocytes become harmful: functional and inflammatory responses that contribute to Alzheimer's disease. Ageing Res Rev 18:29–40
71. Alam Q, Alam MZ, Mushtaq G, Damanhouri GA, Rasool M, Kamal MA, Haque A (2016) Inflammatory process in Alzheimer's and Parkinson's diseases: Central role of cytokines. Curr Pharm Des 22:541–548
72. Frost GR , Li YM (2017) The role of astrocytes in amyloid production and Alzheimer's disease. Open Biol 7(12)
73. Taib T, Leconte C, Van Steenwinckel J, Cho AH, Palmier B, Torsello E, Lai Kuen R, Onyeomah S et al (2017) Neuroinflammation, myelin and behavior: temporal patterns following mild traumatic brain injury in mice. PLoS One 12:e0184811
74. Zetterstrom M, Sundgren-Andersson AK, Ostlund P, Bartfai T (1998) Delineation of the proinflammatory cytokine cascade in fever induction. Ann N Y Acad Sci 856:48–52
75. Sun M, Brady RD, Wright DK, Kim HA, Zhang SR, Sobey CG, Johnstone MR, O'Brien TJ et al (2017) Treatment with an interleukin-1 receptor antagonist mitigates neuroinflammation and brain damage after polytrauma. Brain Behav Immun 66:359–371
76. Lu KT, Wang YW, Yang JT, Yang YL, Chen HI (2005) Effect of interleukin-1 on traumatic brain injury-induced damage to hippocampal neurons. J Neurotrauma 22:885–895
77. Sticozzi C, Belmonte G, Meini A, Carbotti P, Grasso G, Palmi M (2013) IL-1beta induces GFAP expression in vitro and in vivo and protects neurons from traumatic injury-associated apoptosis in rat brain striatum via NFkappaB/Ca(2)(+)-calmodulin/ERK mitogen-activated protein kinase signaling pathway. Neuroscience. 252: 367–383
78. Fields J, Cisneros IE, Borgmann K, Ghorpade A (2013) Extracellular regulated kinase 1/2 signaling is a critical regulator of interleukin-1beta-mediated astrocyte tissue inhibitor of metalloproteinase-1 expression. PLoS One 8:e56891
79. Cheng P, Alberts I, Li X (2013) The role of ERK1/2 in the regulation of proliferation and differentiation of astrocytes in developing brain. Int J Dev Neurosci 31:783–789
80. Sun J, Nan G (2017) The extracellular signal-regulated kinase 1/2 pathway in neurological diseases: a potential therapeutic target (review). Int J Mol Med 39:1338–1346
81. Rama Rao KV, Jayakumar AR, Tong X, Alvarez VM, Norenberg MD (2010) Marked potentiation of cell swelling by cytokines in ammonia-sensitized cultured astrocytes. J Neuroinflammation 7: 66–2094-7-66
82. Mori T, Wang X, Aoki T, Lo EH (2002) Downregulation of matrix metalloproteinase-9 and attenuation of edema via inhibition of ERK mitogen activated protein kinase in traumatic brain injury. J Neurotrauma 19:1411–1419
83. Hui H, Rao W, Zhang L, Xie Z, Peng C, Su N, Wang K, Wang L et al (2016) Inhibition of Na(+)-K(+)-2Cl(−) cotransporter-1 attenuates traumatic brain injury-induced neuronal apoptosis via regulation of Erk signaling. Neurochem Int 94:23–31
84. Yang Z, Fan R, Sun P, Cui H, Peng W, Luo J, Zhang C, Xiong X et al (2018) Rhubarb attenuates cerebral edema via inhibition of the extracellular signal-regulated kinase pathway following traumatic brain injury in rats. Pharmacogn Mag 14:134–139
85. van der Knaap MS, Boor I, Estevez R (2012) Megalencephalic leukoencephalopathy with subcortical cysts: chronic white matter oedema due to a defect in brain ion and water homoeostasis. Lancet Neurol 11:973–985
86. Liu S, Zhu S, Zou Y, Wang T, Fu X (2015) Knockdown of IL-1beta improves hypoxia-ischemia brain associated with IL-6 up-regulation in cell and animal models. Mol Neurobiol 51:743–752
87. Eng LF, Ghirnikar RS (1994) GFAP and astrogliosis. Brain Pathol 4:229–237
88. Ceyzeriat K, Abjean L, Carrillo-de Sauvage MA, Ben Haim L, Escartin C (2016) The complex STATes of astrocyte reactivity: how are they controlled by the JAK-STAT3 pathway? Neuroscience. 330:205–218
89. Toutounchian JJ, McCarty JH (2017) Selective expression of eGFP in mouse perivascular astrocytes by modification of the Mlc1 gene using T2A-based ribosome skipping. Genesis. 55. https://doi.org/10.1002/dvg.23071
90. Estevez R, Elorza-Vidal X, Gaitan-Penas H, Perez-Rius C, Armand-Ugon M, Alonso-Gardon M, Xicoy-Espaulella E, Sirisi S et al (2018) Megalencephalic leukoencephalopathy with subcortical cysts: a personal biochemical retrospective. Eur J Med Genet 61:50–60
91. Sirisi S, Elorza-Vidal X, Arnedo T, Armand-Ugon M, Callejo G, Capdevila-Nortes X, Lopez-Hernandez T, Schulte U et al (2017) Depolarization causes the formation of a ternary complex between GlialCAM, MLC1 and ClC-2 in astrocytes: implications in megalencephalic leukoencephalopathy. Hum Mol Genet 26:2436–2450
92. Dubey M, Brouwers E, Hamilton EMC, Stiedl O, Bugiani M, Koch H, Kole MHP, Boschert U et al (2018) Seizures and disturbed brain potassium dynamics in the leukodystrophy megalencephalic leukoencephalopathy with subcortical cysts. Ann Neurol 83:636–649
93. Tzour A, Leibovich H, Barkai O, Biala Y, Lev S, Yaari Y, Binshtok AM (2017) KV 7/M channels as targets for lipopolysaccharide-induced inflammatory neuronal hyperexcitability. J Physiol 595: 713–738

94. Neprasova H, Anderova M, Petrik D, Vargova L, Kubinova S, Chvatal A, Sykova E (2007) High extracellular K(+) evokes changes in voltage-dependent K(+) and Na (+) currents and volume regulation in astrocytes. Pflugers Arch 453:839–849
95. Okazaki R, Doi T, Hayakawa K, Morioka K, Imamura O, Takishima K, Hamanoue M, Sawada Y et al (2016) The crucial role of Erk2 in demyelinating inflammation in the central nervous system. J Neuroinflammation 13:235–016-0690-8
96. Hamilton EMC, Tekturk P, Cialdella F, van Rappard DF, Wolf NI, Yalcinkaya C, Cetincelik U, Rajaee A et al (2018) Megalencephalic leukoencephalopathy with subcortical cysts: characterization of disease variants. Neurology. 90:e1395–e1403